On perfectly matched layer schemes in finite difference simulations of acoustic Logging-While-Drilling

Hua Wang, Sate Key Lab of Petroleum Resource and Prospecting, China Univ. of Petroleum-Beijing and Earth Resource Lab, MIT; Xuefeng Shang, Xinding Fang, Earth Resource Lab, MIT; Guo Tao, Sate Key Lab of Petroleum Resource and Prospecting, China Univ. of Petroleum-Beijing*

Summary

In the wave propagation simulation by finite difference time domain (FDTD), the perfectly matched layer (PML) is often applied to eliminate the reflection artifacts due to the truncation of the finite computational domain. In the acoustic Logging-While-Drilling (LWD) FDTD simulation, due to high impedance contrast between the drill collar and fluid in the borehole, the stability and efficiency of PML scheme is critical to simulate complicated wave modes accurately. In this paper, we compare four different PML implementations in FDTD in the acoustic LWD simulation, including splitting PML (SPML), Multi-axis PML (MPML), Non-splitting PML (NPML), and complex frequency-shifted PML (CFS-PML). The simulation indicates that NPML and CFS-PML can more efficiently absorb the guide wave reflection from the computational boundaries than SPML and MPML. For large simulation time, SPML, MPML and NPML are numerically instable. However, stability of MPML can be improved further to some extent. Among all, CFS-PML is the best choice for LWD modeling. The effects of CFS-PML parameters on the absorbing efficiency are investigated, including damping profile, frequency-shifted factor, scaling factor and PML thickness. For a typical LWD case, the best value for maximum of quadratic damping profile d_0 is about 1. The optimal parameter space for the maximum value of linear frequency-shifted factor α_0 and scaling factor β_0 depends on the PML damping profile and thickness. If the PML thickness is 10 grids, the reflection residual can be reduced to less than 1%, using optimal CFS-PML parameters, while only about 0.5‰ reflection artifacts are observed for 20 grids PML buffer.

Introduction

Acoustic LWD has been one of hot research areas in exploration geophysics recently. Numerical simulations can help us understand the characteristics of the complicated wave field. Wave number integration (e.g. Wang and Tao, 2011) and finite difference schemes (e.g. Huang, 2003; Wang and Tang, 2003; Wang et al., 2009) are commonly used methods to simulate acoustic logging wave field. The former is fast but can only deal with axial symmetric model. On the other hand, finite difference method, can handle general spatial variations of elastic properties, such as tool isolation design (e.g. Chen et al., 1998; Wang and Tao, 2009) and acoustic LWD tool eccentricity (e.g. Huang, 2003).

To avoid the artificial reflected energy from computational domain boundaries, PML (Bérenger, 1994) is introduced as absorbing boundary layers, which is superior to traditional absorbing boundary condition (ABC) methods. Compared to wire-line case, the acoustic LWD simulation requires PML with higher absorbing efficiency to capture the rich and subtle features in the late arrivals. In the paper, FDTD simulations in acoustic LWD case are presented for different PML implementations, in which the borehole wave modes are very complicated. Firstly, the merits and demerits of different PMLs are compared. Then the optimal parameters of CFS-PML in typical LWD cases are also explored.

PML Theory for Elastic Wave Equation

The stress-velocity scheme of elastic wave equations in Cartesian coordinate (x, y, z) is as following,

$$\frac{\partial \mathbf{v}}{\partial t} = \frac{1}{\rho}\nabla \cdot \boldsymbol{\sigma}, \tag{1a}$$

$$\frac{\partial \boldsymbol{\sigma}}{\partial t} = \mathbf{c} : [\nabla \mathbf{v} + (\nabla \mathbf{v})^T], \tag{1b}$$

where $\mathbf{v}$ is the particle velocity vector, $\boldsymbol{\sigma}$ is the stress tensor, ρ is the density of medium, and $\mathbf{c}$ is the stiffness tensor.

With a complex stretch factor, for instance in x direction, $S_x = 1 + \frac{d_x(x)}{i\omega}$ (Bérenger, 1994; Chew and Liu, 1996), the governing equation in PML region is similar to equation (1), except that the space derivative $\frac{\partial}{\partial x}$ is stretched to $\frac{1}{S_x}\frac{\partial}{\partial x}$. Here, $d_x(x)$ is the damping function and ω is angular frequency. In such a configuration, the incident plane wave along x direction can be exponentially attenuated in the PML region. To avoid convolution operation, in the SPML, each velocity and stress component is split further into parallel and perpendicular components with respect to the coordinate directions (Collino, 2001; Wang et al., 2009).

To improve the stability of SPML, Meza-Fajardo et al. (2008) analyzed the numerical stability of SPML and introduce a modified version, MPML, in which damping in different direction is coupled. Taking x direction for example, the damping profile $d_x(x)$ is modified as $d_x(x) = d_x^x(x) + p_{yx}d_x^x(x) + p_{zx}d_x^x(x)$, where $d_x^x(x)$ can

derived from SPML, and the p_{yx} and p_{zx} are correction coefficients that can be tuned according to specific cases.

The two main drawbacks in SPML and MPML are: 1) the large memory requirement due to the wave field splitting in PML region; 2) the poor absorbing performance for grazing incident wave because only the normal component of the incident wave is attenuated in SPML and MPML. Wang and Tang (2003) introduced non-splitting PML (NPML), in which a trapezoidal rule (time accuracy is second order) is applied to calculate the convolutions in PML formula.

In order to absorb evanescent waves and guide waves efficiently, Roden and Gendney (2000) proposed a general stretch factor $S = \beta + \frac{d}{\alpha + i\omega}$ for CFS-PML, where α is frequency-shifted factor and β is a scaling factor. Komatitch et al. (2007) used recursive convolution method to implement the CFS-PML with FDTD. Zhang and Shen (2010) used auxiliary differential equations (ADE) method to attain higher order time accuracy. All of the PML methods described above are summarized in Table 1.

Table 1: Summary of PML

	SPML	MPML	NPML	CFS-PML
α	0	0	0	Non-zero
β	1	1	1	Variable
d_x	d_x^x	$(1+p_{yx}+p_{zx})\,d_x^x$	d_x^x	d_x^x
Convolution	No	No	Yes	Yes

In general, the damping profile is chosen as a polynomial function. Here we follow Collino's equation (Collino and Tsogka, 2001), for the damping along x direction:

$$d_x = d_0\left(\frac{l_x}{L}\right)^n \qquad (2)$$

where l_x is distance from PML-interior interface, n is 2 in this paper and d_0 is the maximum value of d, and L is the thickness of PML layer.

The value of α and β in CFS-PML are usually given by the following polynomials (e.g. Komtatitsch et al., 2007),

$$\beta_x = 1 + (\beta_0 - 1)\left(\frac{l_x}{L}\right)^m, \qquad (3)$$

$$\alpha_x = \alpha_0\left(1 - (\frac{l_x}{L})^p\right), \qquad (4)$$

where we choose m and p as 2 and 1, respectively, and α_0 and β_0 are the maximum values of α and β.

Acoustic LWD System and Medium Parameters

The model of the borehole and LWD tool configuration is illustrated in Figure 1 and the tool/model parameters are listed in Table 2.

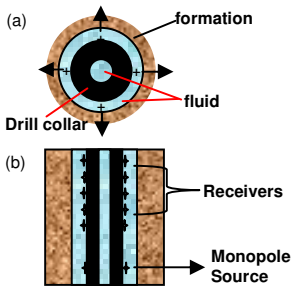

Figure 1: Schematic diagram of model and the location of source and receivers. (a) Top view of the model, and vibration modes of sources are indicated by arrows. (b) Schematic diagram of x-z cross-section. x is along horizontal direction, and z is vertical direction.

Table 2: Parameters of tool and formation

	$V_p(m/s)$	$V_s(m/s)$	$Density(g/cm^3)$	$Radius(mm)$
Inner Fluid	1470	—	1.00	27
Drill collar	5860	3130	7.85	90
Outer Fluid	1470	—	1.00	117
Formation	3927	2455	2.32	∞

Computational Results and Discussion

Firstly, we implement the four different PMLs in 2D LWD case for the model shown in Figure 1b. Staggered grid FDTD scheme is used with 4th order space accuracy and 2nd order in time (Tao et al., 2008). The model is discretized into 123 by 334 grids along x- and z- direction respectively. The grid spacing is 9mm, and time step is 0.9μs. The PML layer thickness is 20 grids. A monopole source is applied and the source time function is a Ricker wavelet with central frequency f_c as 10 kHz. d_0, α_0 and β_0 are chosen as 1, πf_c and 7 respectively. The results are demonstrated in Figure 2.

In case of SPML (Figure 2a), drill collar wave, shear (S) wave, and Stoneley (St.) wave can be easily identified from the arrival time. Also, the artificial reflection from boundaries (dash black line) is visible, which is reflected St. wave by time semblance method (Kimball and Marzetta, 1986). The simulation becomes unstable after 10 ms, indicating ill-posed nature of SPML scheme in LWD case.

Figure 2b shows the result of MPML with correction coefficients p_{zx} and p_{xz} taken as 0.1. The reflection artifacts are still visible, whereas the instability issue is improved to some extent (it appears after 13 ms).

Comparing figures 2a to 2c, NPML (Figure 2c) is superior to SPML and MPML in suppressing reflected St. wave. However, the intrinsic instability of NPML (after 12 ms in

Figure 2c) in LWD case indicates that it is not suitable for large simulation time.

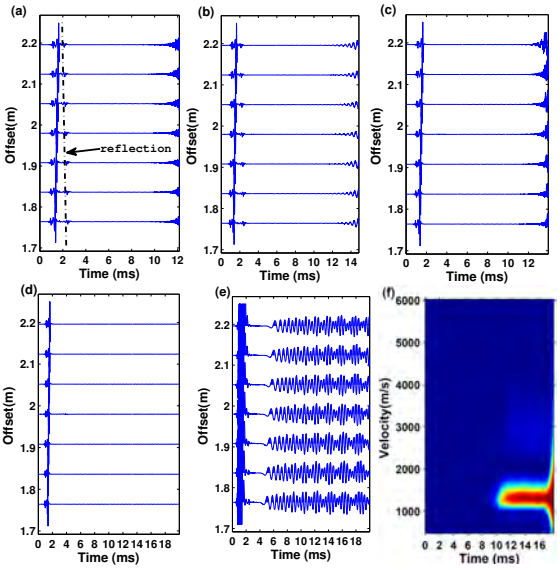

Figure 2: Waveform of array receivers in LWD case. (a) Result of SPML; (b) Result of MPML;(c) Result of NPML;(d) Result of ADE CFS-PML; (e) Waveform zoomed in by 100 times of (d); (f) Velocity-time analysis of the array waveform after 4ms of figure (e)

Ineffectiveness to evanescent and instability in long time simulation are reported in electromagnetic wave simulation (Bérenger, 1997) by FDTD with conventional PML (Bérenger, 1994). Kuzuoglu and Mittra (1996) analyzed the causality of conventional PML and found that the conventional stretch factor does not meet the causality. They introduced CFS-PML where they use a modified factor $S = 1 + \frac{d}{1 + i\omega}$. In this case, the pole is moved from the real axis to the complex plane. The conventional PML (Bérenger, 1994) is a high frequency approximate solution of CFS-PML and does not perform well for low frequencies. Abarbanel and Gottlieb (1997) proved that the conventional PML is only weakly well-posed and would diverge under small perturbations. Due to this, instable signals appear in large simulation time (Figure 2a to 2c).

We implement the CFS-PML (Figure 2d) with the ADE method (Zhang and Shen, 2010). Obviously, CFS-PML is the winner among the four in the sense of stability and absorbing efficiency. The coda after 4 *ms* are zoomed in by 100 times (Figure 2e), and can be identified as reflected St. wave by time semblance (Figure 2f). In the LWD FDTD simulation, the main source of PML artifacts is guide wave (e.g. St. wave). The parameters of CFS-PML can be finely tuned to optimize the absorption of the guide waves, which is discussed in the next section.

CFS-PML Parameter optimization in LWD Simulation

The effects of CFS-PML parameters on the absorption efficiency have been discussed based on homogenous models (e.g. Komatitsch, 2007; Zhang and Shen, 2010). Here we optimize the parameters specifically for the LWD simulation. The computational domain for 3D model is 30 *cm* by 30 *cm* by 20 *cm* (shown in Figure 1). The media parameters and borehole geometry are defined in Table 2. The space grid size is 5*mm*; time step is 0.4μs and total simulation time is 2 *ms*. Thousands of simulations are performed, using different PML parameter combinations. Here d_0, α_0, β_0 and L are considered. A very large model is chosen as a reference model, in which no reflected energy from the boundaries appears in the first 2 *ms* time window. The global error is defined as:

$$E_g = \frac{\sum_t \left| P_{PML}(t) - P_{ref}(t) \right|}{\sum_t \left| P_{ref}(t) \right|}, \qquad (5)$$

where E_g is global error of a given PML model, P_{PML} and P_{ref} are the pressure field of the PML model and reference model respectively, and t is time. The global errors are shown in Figure 3 and Figure 4, for different d_0, α_0, β_0 and L.

As shown in Figure 3, the global error changes with d_0. And the minimum global error is less than 1% when d_0 is 1, while others are lager than that or have less space than that. It can be drawn that the best value of d_0 is 1. This differs from the result of Zhang and Shen (2010) due to the inhomogeneous model in LWD case. At the same time, we can also find that the optimal value of β_0 is between 6 and 13, and the best combination of α_0 and β_0 is about 1.5 and 10 from Figure 3(b). Even here, we observe some deviation from empirical formula for β_0 suggested by Zhang and Shen (2010). Therefore, the empirical formula of β_0 should be modified in inhomogeneous model such as LWD case.

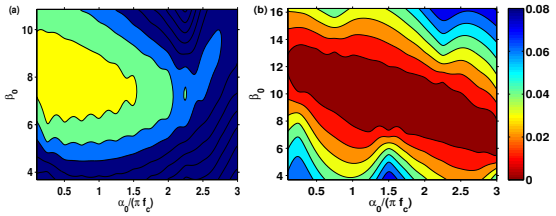

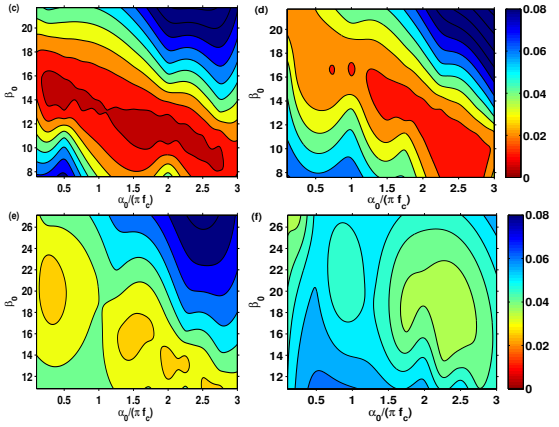

Figure 3 Contours of global error with α_0, β_0 and d_0 variation (L=10).(a) Contours of global error as function of α_0, and β_0 with d_0 equal to 0.5; (b) Contours of global error as function of α_0, and β_0 with d_0 equal to 1; (c) Contours of global error as function of α_0, and β_0 with d_0 equal to 1.5; (d) Contours of global error as function of α_0, and β_0 with d_0 equal to 2; (e) Contours of global error as function of α_0, and β_0 with d_0 equal to 2.5; (f) Contours of global error as function of α_0, and β_0 with d_0 equal to 3

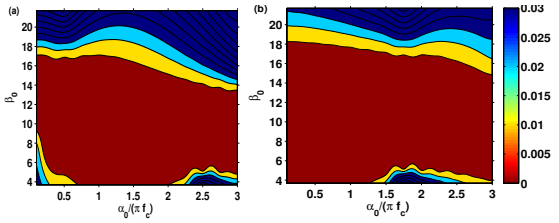

Figure 4 Contours of global error with α_0, β_0 and L variation (d_0=1). (a) Contours of global error as function of α_0, and β_0 with L equal to 20; (b) Contours of global error as function of α_0, and β_0 with L equal to 30

The effect of thickness of PML on global error with d_0=1 is also discussed in the paper, as shown in Figure 4. Combining Figure 4 with Figure 3(b), we can find that the global error decreases as L increase, and the range of optimal α_0 and β_0 become larger. Increasing PML thickness to 20 grids, we can get a reflectivity of PML 5‰ for a large range of α_0 and β_0. This indicates the excellent performance of CFS-PML.

Conclusions

Four kinds of PML are implemented in FDTD in the 2D acoustic LWD simulation. The simulation indicates that NPML and CFS-PML can more efficiently absorb the guide wave reflection from the computation boundaries than SPML and MPML. For long time simulation, the numerical instability is observed in SPML, MPML and NPML, though MPML can improve the stability to some extent. Among of all, CFS-PML is the best choice for LWD simulation.

The effects of CFS-PML parameters on the absorbing efficiency are investigated based on thousands of 3D simulations. For a typical LWD case, the best maximum value of quadratic damping profile d_0 is about 1. The optimal parameter space for the maximum value of linear frequency-shifted factor α_0 and scaling factor β_0 depends on the PML damping profile and thickness. If the PML thickness is 10 grids, the reflection residual can be reduced to less than 1%, using optimal PML parameters, while only less than 0.5% reflection artifacts are observed given the PML thickness is 20.

Acknowledgments

This study is supported by the National Major Fundamental Research Program of China (Grant No.2007CB209601), a National 863 Project (NO.2006AA06Z207) and one of the major state S&T special projects (NO. 2008ZX05000-020). Hua Wang would like to thank the support from China Scholarship Council (NO.2010644006).

EDITED REFERENCES

Note: This reference list is a copy-edited version of the reference list submitted by the author. Reference lists for the 2011 SEG Technical Program Expanded Abstracts have been copy edited so that references provided with the online metadata for each paper will achieve a high degree of linking to cited sources that appear on the Web.

REFERENCES

Abarbanel, S., and D. Gottlieb, 1997, A mathematical analysis of the PML method: Journal of Computational Physics, **134**, no. 2, 357–363, doi:10.1006/jcph.1997.5717.

Bérenger, J. P., 1994, A perfectly matched layer for the absorption of electromagnetic waves: Journal of Computational Physics, **114**, no. 2, 185–200, doi:10.1006/jcph.1994.1159.

———, 1997, Improved PML for the FDTD solution of wave-structure interaction problems: IEEE Transactions on Antennas and Propagation, **45**, no. 3, 466–473, doi:10.1109/8.558661.

Chen, Y., W. Chew, and Q. Liu, 1998, A three-dimensional finite difference code for the modeling of sonic logging tools: Journal of the Acoustical Society of America, **103**, no. 2, 702–712, doi:10.1121/1.421230.

Chew, W., and Q. Liu, 1996, Perfectly matched layers for elastodynamics: A new absorbing boundary condition: Journal of Computational Acoustics, **4**, no. 4, 341–359, doi:10.1142/S0218396X96000118.

Collino, F., and C. Tsogka, 2001, Application of the perfectly matched absorbing layer model to the linear elastodynamic problem in anisotropic heterogeneous media: Geophysics, **66**, 294–307, doi:10.1190/1.1444908.

Huang, X. J., 2003, Effects of tool position on borehole acoustic measurements: A stretched grid finite difference approach: Ph.D. thesis, Massachusetts Institute of Technology.

Kimball, C. V., and T. Marzetta, 1984, Semblance processing of borehole acoustic array data: Geophysics, **49**, 274–281, doi:10.1190/1.1441659.

Komatitsch, D., and R. Martin, 2007, An unsplit convolutional perfectly matched layer improved at grazing incidence for the seismic wave equation: Geophysics, **72**, no. 5, SM155–SM167, doi:10.1190/1.2757586.

Kuzuoglu, M., and R. Mittra, 1996, Frequency dependence of the constitutive parameters of causal perfectly matched anisotropic absorbers: IEEE Microwave and Guided Wave Letters, **6**, no. 12, 447–449, doi:10.1109/75.544545.

Meza-Fajardo, K. C., and A. S. Papageorgiou, 2008, A nonconvolutional, split-field, perfectly matched layer for wave propagation in isotropic and anisotropic elastic media: Stability analysis: Bulletin of the Seismological Society of America, **98**, no. 4, 1811–1836, doi:10.1785/0120070223.

Roden, J. A., and S. D. Gedney, 2000, Convolution PML (CPML): An efficient FDTD implementation of the CFS-PML for arbitrary media: Microwave and Optical Technology Letters, **27**, no. 5, 334–339, doi:10.1002/1098-2760(20001205)27:5<334::AID-MOP14>3.0.CO;2-A.

Tao, G., F. He, B. Wang, H. Wang, and P. Chen, 2008, Study on 3D simulation of wavefields in acoustic reflection image logging: Science China D-Earth, **51**, S2, 186–194, doi:10.1007/s11430-008-6009-6.

Wang, H., and G. Tao, 2011, Wavefield simulation and data-acquisition-scheme analysis for LWD acoustic tools in very slow formations: Geophysics, **76**, no. 4, B1–B10.

Wang, H., G. Tao, B. Wang, W. Li, and X. Zhang, 2009, Wavefield simulation and data acquisition scheme analysis for LWD acoustic tool: Chinese Journal of Geophysics, **52**, no. 9, 2402–2409, in Chinese.

Wang, T., and X. Tang, 2003, Finite-difference modeling of elastic wave propagation: A nonsplitting perfectly matched layer approach: Geophysics, **68**, 1749–1755, doi:10.1190/1.1620648.

Zhang, W., and Y. Shen, 2010, Unsplit complex frequency-shifted PML implementation using auxiliary differential equations for seismic wave modeling: Geophysics, **75**, no. 4, T141–T154, doi:10.1190/1.3463431.